Receptance based approach for control of floor vibrations

Donald Steve Nyawako[1*], Maryam Ghandchi Tehrani[2], Paul Reynolds[3]

[1,3]*Vibration Engineering Section, College of Engineering, Mathematics and Physical Sciences, University of Exeter, North Park Road, Exeter, EX4 4QF, UK.*
[2]*Institute of Sound and Vibration Research, University of Southampton, Highfield, Southampton, SO17 1BJ, UK.*

ABSTRACT

Advances in design, materials and construction technologies, coupled with client and architectural requirements, are some of the drivers for light-weight and slender pedestrian structures, which are becoming increasingly susceptible to human induced vibrations. The use of active control techniques is progressively being viewed as a more feasible approach for suppressing such vibrations compared with traditional passive technologies. In this paper, the principles of the receptance based approach are exploited to design appropriate feedback gains that place the eigenvalues of selected vibration modes of an experimental footbridge structure at selected locations thereby enhancing its vibration performance. These studies are based on a single-input multiple-output (SIMO) controller structure comprising of a single control actuator and two sensors. It is seen that this has the potential to offer additional design freedoms beyond purely a direct velocity feedback (DVF) controller. A comparative study is carried out with a DVF controller implemented in a single-input single-output (SISO) scheme. This work presents the analytical determination of appropriate feedback gains from results of experimental modal analysis (EMA) on the structure and thereafter the experimental implementation of these feedback gains. Vibration mitigation performance is evaluated through both changes in measured transfer functions and reductions in response under single pedestrian excitation.

Keywords: *Vibration control, receptance method, velocity feedback*

1 INTRODUCTION

Advances in design, materials and construction technologies, coupled with client and architectural requirements are emerging as the primary drivers for light-weight and slender pedestrian structures. These are characterised by low modal frequencies and damping ratios making them increasingly susceptible to human induced vibrations. The use of active control techniques is progressively being viewed as a more feasible approach for improving their vibration serviceability performance in comparison with more traditional passive technologies. This is taking into account both vibration mitigation improvements achievable as well the intrusiveness imposed by various vibration control technologies. There are, however, other more complex factors like installation and running costs that should be considered in any practical application.

The performance of active vibration control systems for control of pedestrian induced vibration has been investigated in a number of previous studies [1,2,3,4]. The common feature in most of the studies is the use of the velocity feedback control scheme. It has been employed to augment damping in these structures, thereby improving their dynamic response when subjected to human induced vibrations. Appropriate compensation has also been provided to the electromagnetic proof-mass

---

1 Postdoctoral Research Fellow, D.S.Nyawako@exeter.ac.uk

2 Lecturer in Active Control, M.Ghandchi-Tehrani@soton.ac.uk

3 Professor of Structural Dynamics and Control, P.Reynolds@exeter.ac.uk

* Corresponding author

(inertial) actuators used. One of the primary benefits of the direct velocity feedback controller is that it is an active damping strategy that can quickly be tuned to provide desirable vibration mitigation performance.

Eigenvalue assignment problems have been extensively researched by the wider control community since studies presented by [5], in which it was demonstrated that all the poles of the system could be assigned by state feedback if the system was controllable. Additionally, the key requirements under which output feedback could be used for eigenvalue assignment were outlined by [6]. It is the motivation from such earlier studies as well as subsequent studies that the receptance based technique was also developed for addressing pole/zero assignment problems. The theory behind the receptance approach has been introduced using both state feedback [7] and output feedback [8] control strategies in both single-input multiple-output (SIMO) and multiple-input multiple-output (MIMO) structures. This design approach has also been exploited to realise additional vibration mitigation objectives such as partial pole placement [9,10]. One of its primary advantages is that it can be implemented on measured vibration data. In past studies, the design approach has entailed the determination of appropriate feedback gain terms (displacement and velocity) that achieve the desired closed-loop characteristics of the system's eigenvalues. It is seen in these previous research studies that it offers greater flexibilities for achieving a wide array of vibration mitigation objectives as seen in some experimental implementations on both a T-shaped plate prototype and a modular test structure (H-shaped).

In the work presented here, the receptance based controller design approach is exploited to design appropriate feedback gains (velocity and acceleration) that place the open-loop eigenvalues of the first two vibration modes of a footbridge structure at prespecified locations using output feedback control. The work presented here comprises of both analytical predictions using a derived reduced order model (ROM) of the structure as well as experimental results from implementation of the designed feedback gains. For the receptance based controller, the controller structure adopts a single-input multiple-output (SIMO) strategy that makes use of two sensors and a single control actuator. One of the sensors is collocated with the control actuator. The DVF controller is implemented in a single-input single-output (SISO) scheme with a collocated actuator and sensor pair.

2   TEST STRUCTURE AND MODAL MEASUREMENTS

The test structure is a prototype footbridge built under laboratory conditions as shown in Fig. 1. It comprises of two primary beams of size 457x191x82 UB spanning 15.0 m and two edge beams of size 203x203x46 UC spanning 2.5 m. The primary beams rest on knife-edge supports at the four corners. The decking consists of twelve 1.25 m x 2.5 m sandwich plate system (SPS) plates that are bolted to the primary beams. Continuity between them is provided by 200x12 plates, approximately 2.5 m in length and bolted underneath the SPS plates.

Figure 1 – Prototype footbridge structure in VES Labs, University of Exeter

Three APS Dynamics electrodynamic shakers (2x Model 400 and 1x Model 113-HF), were used to excite the structure. These were placed at test points (TPs) 3, 16 and 23 as shown in Fig. 2.

The shakers were driven by statistically uncorrelated random signals so that the FRFs corresponding with individual shakers could be evaluated. The shaker forces were measured using Endevco 7754A-1000 accelerometers that were attached to the inertial masses.

Responses were measured using an array of 9 Honeywell QA750 servo accelerometers that were mounted on levelled Perspex base plates. These were roved three times, i.e. TPs 1-9, 10-18 and 19-27, thereby covering all points on the 27 point test grid. Data acquisition was carried out using a Data Physics Mobilyzer II digital spectrum analyser, which has 24 24-bit input channels and 4 output channels to supply drive signals to the shakers. The force and vibration response data were sampled using a baseband setting of 80 Hz on the spectrum analyser, which corresponds to a sampling rate of 204.8 Hz. All acquisitions were made using a Hanning window and 50% overlap and were averaged to calculate the FRFs. Fig. 3 shows the point acceleration FRFs at the collocated shaker and accelerometer locations.
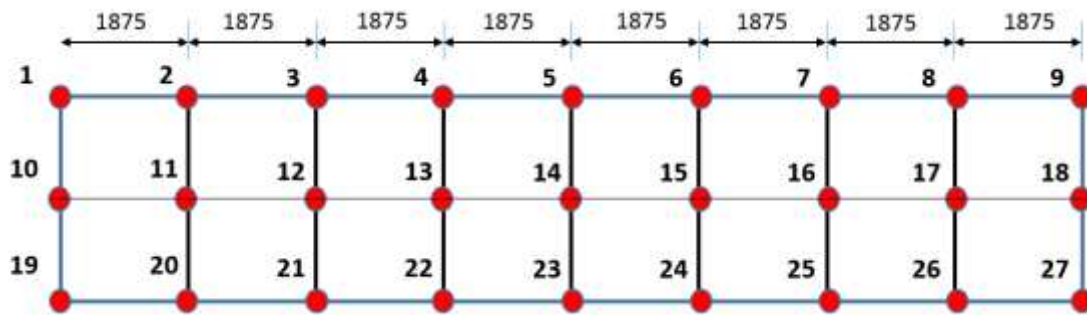

Figure 2 – Test grid used for experimental modal analysis (EMA) tests
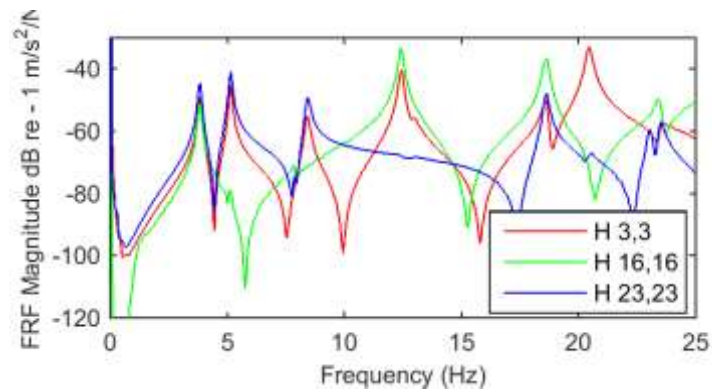

Figure 3 – Point acceleration FRFs at the collocated shaker and accelerometer locations

The FRF data were analysed using the ME'scope suite of parameter estimation software to determine the modal properties (natural frequencies, damping ratios and mode shapes). The test grid used for visualisation of the mode shapes is shown in Fig. 2. The numerical results of the modal parameter estimation are summarised for the first seven modes in Table 1 and the first two vibration mode shapes are shown in Fig. 4.
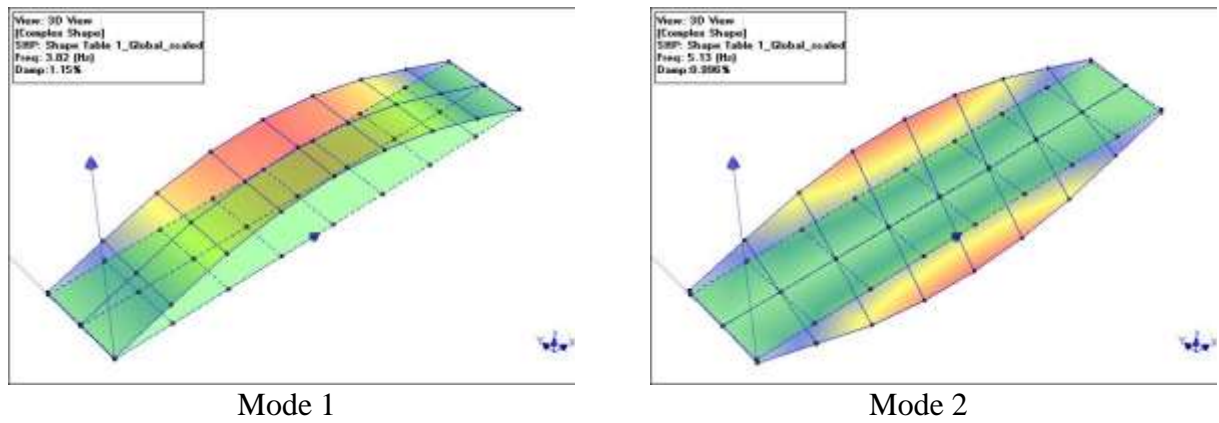
Mode 1   Mode 2

Figure 4 – Mode shapes of the first two vibration modes of the structure

Table 1: Numerical modal properties from footbridge modal tests

Mode	Natural Frequency [Hz]	Damping Ratio [%]
1	3.82	1.2
2	5.13	1.0
3	8.42	1.1
4	12.4	0.6
5	12.9	0.9
6	18.6	0.5
7	20.5	0.6

Fig. 5 shows the point acceleration FRF at TP23 as well as the cross-acceleration FRF between TPs 23 and 3 from the experimental modal analysis tests. Also shown are FRFs relating to the full-order model (FOM) derived from the ME'scope estimates. These are the two locations selected for the SIMO controller studies with receptance based design. In the studies, two sensors are placed at TPs 3 and 23 and the control actuator is placed at TP23.
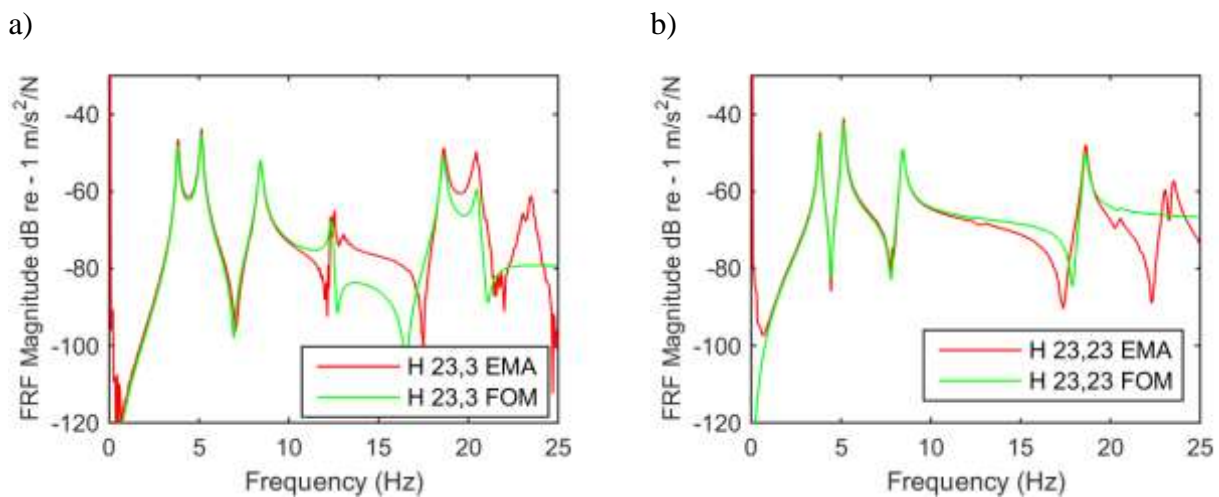
a)   b)

Figure 5 – Cross-accelerance and point accelerance FRFs (a) between TP23 and TP3 (b) at TP23 from EMA tests and FOM based on ME'scope estimates

3 CONTROL DESIGN

Fig. 6 shows a typical feedback control set-up that can be tailored for SISO and SIMO control. $G_p(s)$, $G_{act}(s)$, $G_c(s)$, $G_{not}(s)$, $G_{bp}(s)$ represent the structure, actuator, controller, notch filter and bandpass filter dynamics. $d_i(t)$, $f_c(t)$, $y_a(t)$ and $r(t)$ are the disturbance input force, control force, structural acceleration response and reference input ($r(t)=0$).
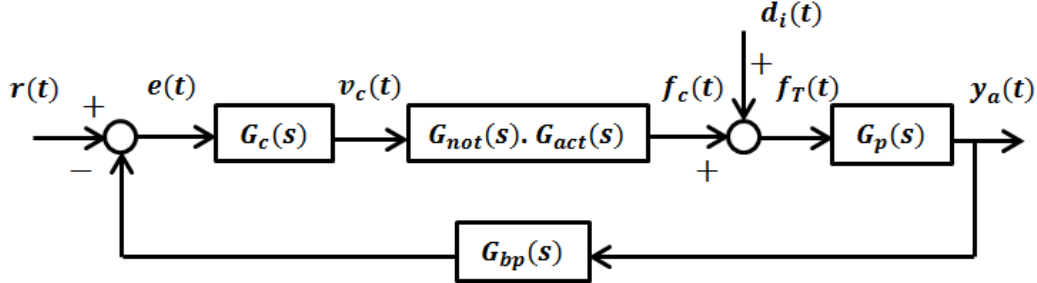

Figure 6 – Feedback control scheme that can be tailored for SISO and SIMO control.

For control of human-induced vibrations, disturbance rejection in Eq. 1 is the primary objective as human walking forces cannot easily be measured. For the DVF controller, $G_c(s)$ is a lossy integrator of the form in Eq. 2 and k_g is the velocity feedback gain. ε is chosen to be very small, typically $\varepsilon \leq 0.01$. For the receptance based design, $G_c(s)$ requires design of velocity and acceleration gains as explained below. The sensitivity of the actuator stroke to human disturbance input can be monitored from Eq. 3 and the notch filter, $G_{not}(s)$, is introduced to compensate for the actuator dynamics. $G_{act\_d}(s)$ represents the actuator displacement to voltage input.

$$Y_a(s) = \frac{G_p(s)}{1+G_p(s)G_{act}(s)G_{not}(s)G_c(s)G_{bp}(s)} \tag{1}$$

$$G_c(s) = \frac{k_g}{s+\varepsilon} \tag{2}$$

$$Y_{act\_d}(s) = \frac{G_{act\_d}(s)G_{not}(s)G_c(s)G_{bp}(s)G_p(s)}{1+G_p(s)G_{act\_d}(s)G_{not}(s)G_c(s)G_{bp}(s)}D_i(s) \tag{3}$$

Stability studies are carried out to evaluate the appropriateness of the designed feedback gains. This involves checks on the following two criteria:

1. System closed-loop stability using the Nyquist contour plot of the closed-loop system $G_{cl\_1}(s)$ for the SISO system with the velocity feedback controller. The closed-loop system is stable provided the Nyquist contour does not encircle the instability point $-1, j0$. For the receptance based controllers, the stability of the closed-loop system is evaluated from the Generalized Nyquist criteria by plotting $\det(G_{cl\_2}(s))$, and this should not encircle the point $0, j0$. Minimum stability margins specified are gain and phase margin of 10dB and 30^0. $G_{cl\_1}(s) = G_p(s)G_{act}(s)G_{not}(s)G_c(s)G_{bp}(s)$, $G_{cl\_2}(s) = 1+(s\mathbf{g}+s^2\mathbf{f})^T \mathbf{H}(s)\mathbf{b}$ and parameters of the latter are defined below.

2. A limit of 0.035 mm/N on the actuator stroke to disturbance input relationship in Eq. 3 around the actuator resonant frequency $(k_1\omega_{act} < \omega_{act} < k_2\omega_{act})$ for $k_1 = 0.5, k_2 = 1.5$ in this work.

The formulation of the receptance based design procedure adopts a similar procedure to that outlined by [7,8,9]. The derivation presented here considers a single-input system. The dynamic equations of a given system expressed in the frequency domain can be shown in Eq. 4, where $\mathbf{M}$, $\mathbf{C}$, and $\mathbf{K}$ are mass, damping and stiffness matrices and $\mathbf{b}$ and $\mathbf{p}$ represent the input and disturbance force vectors. Eq. 5 gives the control force $\mathbf{u}(s)$ in terms of the velocity and acceleration feedback gains $\mathbf{g}$ and $\mathbf{f}$. From Eqs. 4 and 5, it is easily seen how the closed-loop dynamic stiffness in Eq. 6 is altered by the rank-1 matrix $\mathbf{b}(s\mathbf{g} + s^2\mathbf{f})^T$ [7]. The Sherman-Morrison formula gives the inverse of a matrix with a rank-1 modification in terms of the inverse of the original matrix and by using this property, the closed-loop receptance matrix can be expressed as shown in Eq. 7. In theory $\mathbf{H}(s) = (\mathbf{M}s^2 + \mathbf{C}s + \mathbf{K})^{-1}$, whereas in practice $\mathbf{H}(s)$ can be determined from experimental measurements using various actuator and sensor configurations. The characteristic polynomial from Eq. 7 i.e. $1 + (s\mathbf{g} + s^2\mathbf{f})^T \mathbf{H}(s)\mathbf{b}$ is linear in the unknown gains $\mathbf{g}$ and $\mathbf{f}$, and the problem of assignment of the poles of the system can be expressed as shown in Eq. 8. The assigned poles μ_1, μ_2 ,..., μ_{2n} are distinct under closed-loop conjugation. For the output feedback case, with Eq. 9, an additional constraint $\mathbf{D} = \mathbf{b}^T$ can be imposed to enable collocated sensor and actuator pairs.

$$(\mathbf{M}s^2 + \mathbf{C}s + \mathbf{K})\mathbf{x}(s) = \mathbf{b}\mathbf{u}(s) + \mathbf{p}(s) \tag{4}$$

$$\mathbf{x}, \mathbf{p} \in \Re^{n\times 1}; \mathbf{u} \in \Re^{1\times m}; \mathbf{M}, \mathbf{C}, \mathbf{K} \in \Re^{n\times n}; \mathbf{b} \in \Re^{n\times 1}$$

$$\mathbf{u}(s) = -(s\mathbf{g} + s^2\mathbf{f})^T \mathbf{x}(s) \tag{5}$$

$$\mathbf{g}, \mathbf{f} \in \Re^{n\times 1}$$

$$(\mathbf{M}s^2 + \mathbf{C}s + \mathbf{K} + \mathbf{b}(s\mathbf{g} + s^2\mathbf{f})^T)\mathbf{x}(s) = \mathbf{p}(s) \tag{6}$$

$$\hat{\mathbf{H}}(s) = \mathbf{H}(s) - \frac{\mathbf{H}(s)\mathbf{b}(s\mathbf{g} + s^2\mathbf{f})\mathbf{H}(s)}{1 + (s\mathbf{g} + s^2\mathbf{f})^T \mathbf{H}(s)\mathbf{b}} \tag{7}$$

$$\begin{bmatrix} \mu_1\mathbf{r}_1^T & \mu_1^2\mathbf{r}_1^T \\ \mu_2\mathbf{r}_2^T & \mu_2^2\mathbf{r}_2^T \\ \vdots & \vdots \\ \mu_{2n}\mathbf{r}_{2n}^T & \mu_{2n}^2\mathbf{r}_{2n}^T \end{bmatrix} \begin{pmatrix} \mathbf{g} \\ \mathbf{f} \end{pmatrix} = -\begin{pmatrix} 1 \\ 1 \\ \vdots \\ 1 \end{pmatrix}; \mathbf{r}_k = \mathbf{H}(\mu_k)\mathbf{b} \tag{8}$$

$$\mathbf{y}(s) = \mathbf{D}\mathbf{x}(s) \tag{9}$$

For this work, two sensors are located at TPs 3 and 23, and one control actuator is sited at TP23. $\mathbf{H}(s) = \begin{bmatrix} \mathbf{H}_{3,3}(s) & \mathbf{H}_{3,23}(s) \\ \mathbf{H}_{23,3}(s) & \mathbf{H}_{23,23}(s) \end{bmatrix}$ in Eq. 7 is based on the two lowest vibration modes of the structure in Fig. 5 and vector $\mathbf{b} = [0;1]$ to impose control at TP23. Vector $\mathbf{b}$ is selected according to mode shapes of the structure to offer the flexibility of controlling particular vibration modes.

The open loop eigenvalues of the lowest two vibration modes of the structure that are to be augmented by both the receptance-based pole placement and velocity feedback controllers are shown in Table 2.

Table 2: Open loop eigenvalues of vibration modes 1 and 2

Mode	Open loop eigenvalues
1	$-0.28 \pm 24.00i$
2	$-0.32 \pm 32.23i$

A summary of the desired closed-loop eigenvalues of the lowest two vibration modes of the footbridge structure is now presented in Table 3. They are selected to satisfy different design objectives. Controller 1 (M1+M2) augments damping in modes 1 and 2, controller 2 (M2) primarily augments damping in mode 2, and controller 3 (M1) primarily augments damping in mode 1. Based on these design objectives, the gain parameters $\mathbf{g} = [g_1; g_2]$ and $\mathbf{f} = [f_1; f_2]$ in Table 3 that represent velocity and acceleration feedback gains (sensors at TPs 3 and 23) from the receptance-based design approach are obtained. The feedback gains are found to satisfy the stability requirements and an actuator stroke to disturbance input limiter. Also shown in Table 3 are the achieved closed-loop eigenvalues by implementation of the gain terms in the full order model (FOM). These gains satisfy the stability requirements outlined earlier and are implemented in both the numerical studies and experimental implementation.

Table 3: Feedback gain parameters and desired and achieved closed-loop eigenvalues for SIMO controller structure

| Controller	Desired closed-loop eigenvalues	Velocity feedback gains, $\mathbf{g} = [g_1; g_2]$	Acceleration feedback gains, $\mathbf{f} = [f_1; f_2]$	Achieved closed-loop eigenvalues
1 (M1+M2)	$-3.0 \pm 23.8i$ $-3.5 \pm 32.0i$	$[8.0; 76.6]$	$[0.5; -1.1]$	$-3.3 \pm 23.1i$ $-3.5 \pm 31.8i$
2 (M2)	$-0.4 \pm 23.9i$ $-3.9 \pm 32.0i$	$[-79.2; 66.5]$	$[0.9; -0.7]$	$-0.4 \pm 24.0i$ $-4.0 \pm 31.8i$
3 (M1)	$-3.3 \pm 23.8i$ $-0.5 \pm 32.2i$	$[75.7; 61.2]$	$[-1.4; -1.1]$	$-3.3 \pm 23.0i$ $-0.5 \pm 32.2i$

For the DVF controller, a velocity feedback gain of $k_{dvf} = 65$ Vs/m satisfies the stability requirements desired and is implemented in both the numerical studies and experimental implementation.

4 NUMERICAL SIMULATIONS

These studies are based on the FOM of the footbridge structure and they comprise of:

a) Estimates of frequency response functions (FRFs) for both uncontrolled and actively controlled footbridge structure. These are shown in Fig. 7 where the designed feedback gains are implemented on the derived FOM. The DVF controller is implemented in a SISO scheme whilst the receptance based controller is implemented in a SIMO scheme as noted previously. M1 and M2 refer to the controller objectives of targeting modes 1 and 2 independently, whilst M1M2 refers to the objective of targeting both vibration modes 1 and 2 with the receptance design approach. H 23,23 and H 23,3 refer to the collocated and cross-acceleration FRFs.

b) Uncontrolled and controlled responses to synthesized walking excitation forces at TPs 3 and 23 and shown in Fig. 8. These have been estimated by filtering the uncontrolled response measurements from a pedestrian walking on the footbridge structure through the

inverse dynamics at these locations. The results of this set of studies is provided in Fig. 9. The responses are weighted using the W_b weighting function [11] to account for human sensitivity to vibration at different frequencies. The 1s running root mean square (RMS) acceleration responses are also shown and their associated peak values are presented in Table 4. These are defined as the maximum transient vibration value (MTVV) [12]. Again, M1, M2 and M1M2 highlight the design objectives with the receptance-based design of focusing control effort towards mode 1 only, mode 2 only and both modes 1 and 2.
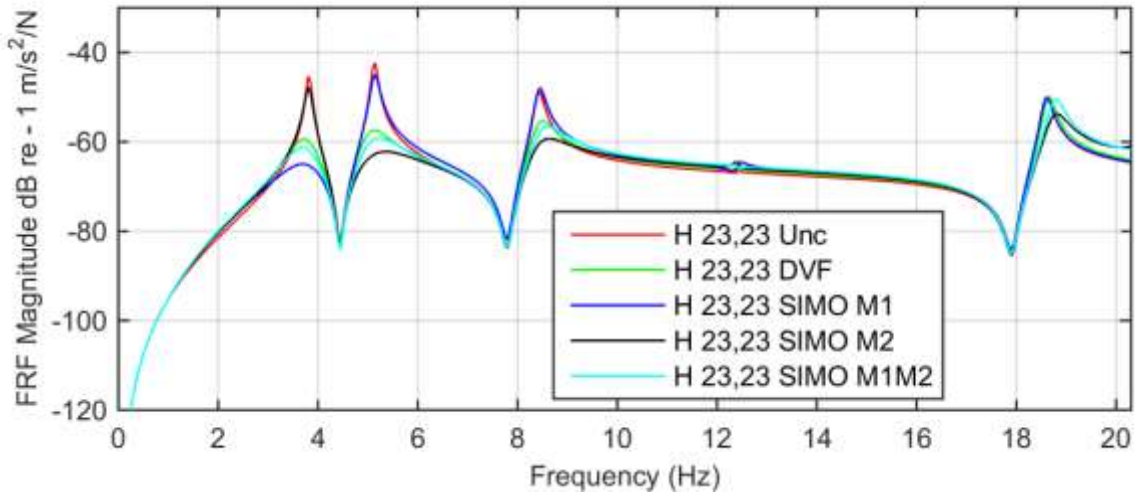
a) FRFs for collocated sensor and actuator pair at TP23
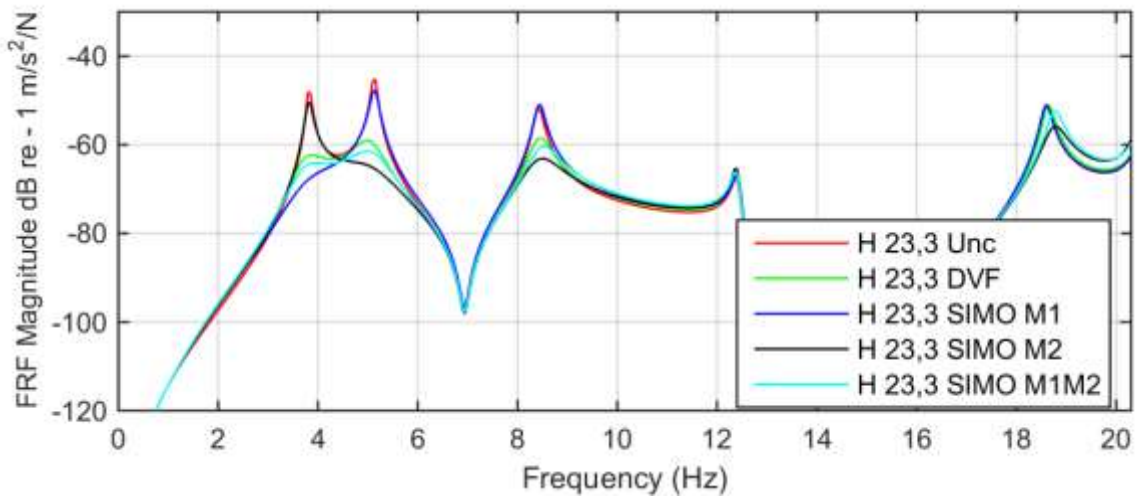
b) Cross FRFs between sensor at TP3 and actuator at TP23

Figure 7 – Estimates of uncontrolled and controlled FRFs for SISO DVF and receptance-based SIMO controllers (actuator at TP23 and two sensor measurements from TPs 3 and 23)
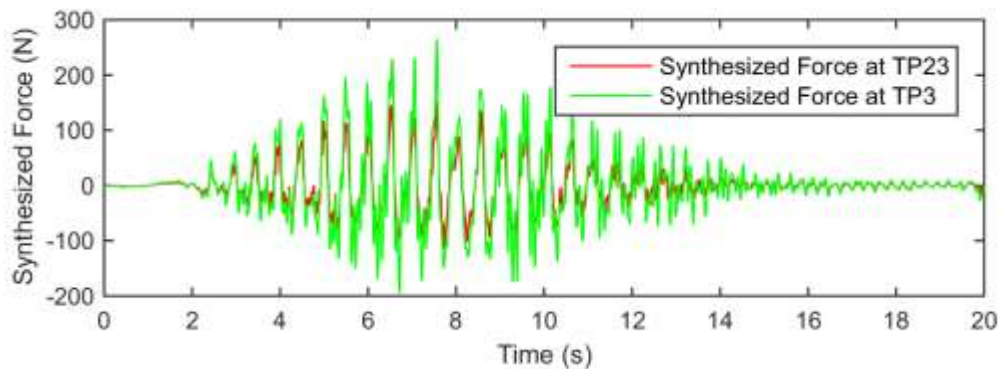
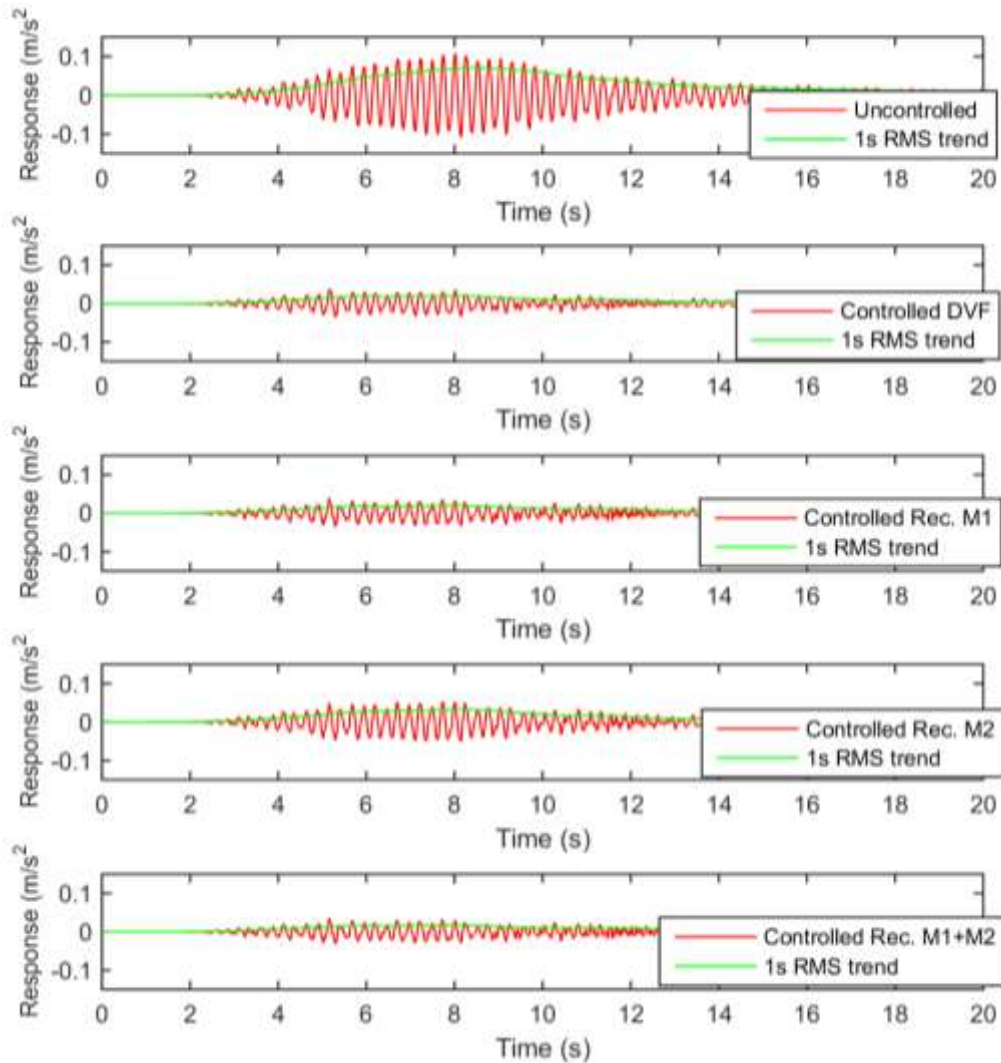*Figure 8 – Synthesized walking forces for the analytical simulations at TPs 3 and 23*

Figure 9 – Uncontrolled and controlled responses from analytical simulations for all responses at TP23

Table 4: Peaks of 1s running RMS acceleration responses for uncontrolled and controlled footbridge under synthesized walking force
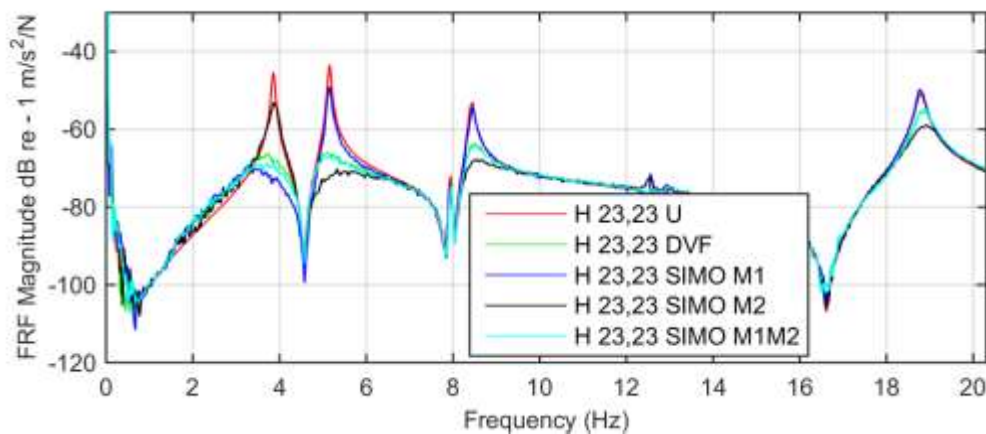
Mode	Acceleration responses at TP23 (m/s^2)	
		% reduction
Uncontrolled	0.0720	
DVF	0.0204	71.7
Receptance M1	0.0209	70.9
Receptance M2	0.0338	53.1
Receptance M1+M2	0.0182	74.7

From the FRF estimates, it can be seen that vibration attenuations of between 15-20 dB are obtained in the target vibration modes. Comparative vibration mitigation performances between the

DVF and receptance based controllers are also seen in Table 4 from the time domain responses to synthesised walking excitation forces. It can be observed that the isolation and control of target resonant frequencies may lead to some degradation in the overall closed-loop performance. This is as a result of walking excitation containing energy not only at the activity frequency but over a broader frequency band.

5 EXPERIMENTAL IMPLEMENTATION

The experimental implementation comprised of a single control shaker sited at TP23 and two sensors sited at TPs 3 and 23. An additional excitation shaker was sited close to TP23 and was used to provide the excitation force for the FRF measurements. For the receptance based controller implementation in the SIMO configuration, the control gains designed in Table 3 were implemented. A DVF controller was also implemented in a SISO configuration for comparative studies. Fig. 10 shows the experimental point and cross accelerance FRFs, which reflect a fairly good correlation with the analytical predictions. Fig. 11 similarly shows the uncontrolled and controlled responses to a pedestrian walking at a pacing rate of 1.93 Hz with the aim of exciting the structure in resonance via the second harmonic of the pacing rate. The responses are also weighted using the weighting function W_b [11]. The 1s running RMS acceleration responses are shown in Fig. 11 and their associated peak values are presented in Table 5.

a)
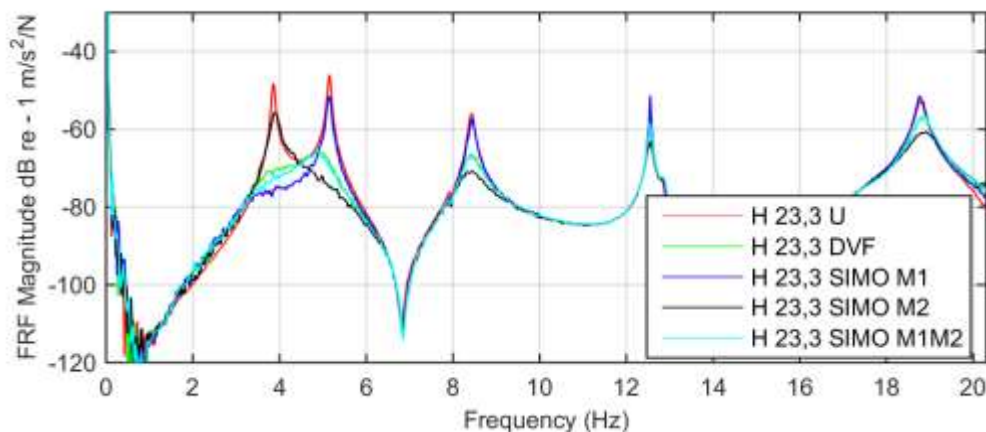
b)

Figure 10 – Uncontrolled and controlled FRFs in experimental studies: (a) at collocated location (TP23) and (b) with reference to non-collocated locations (TP3)
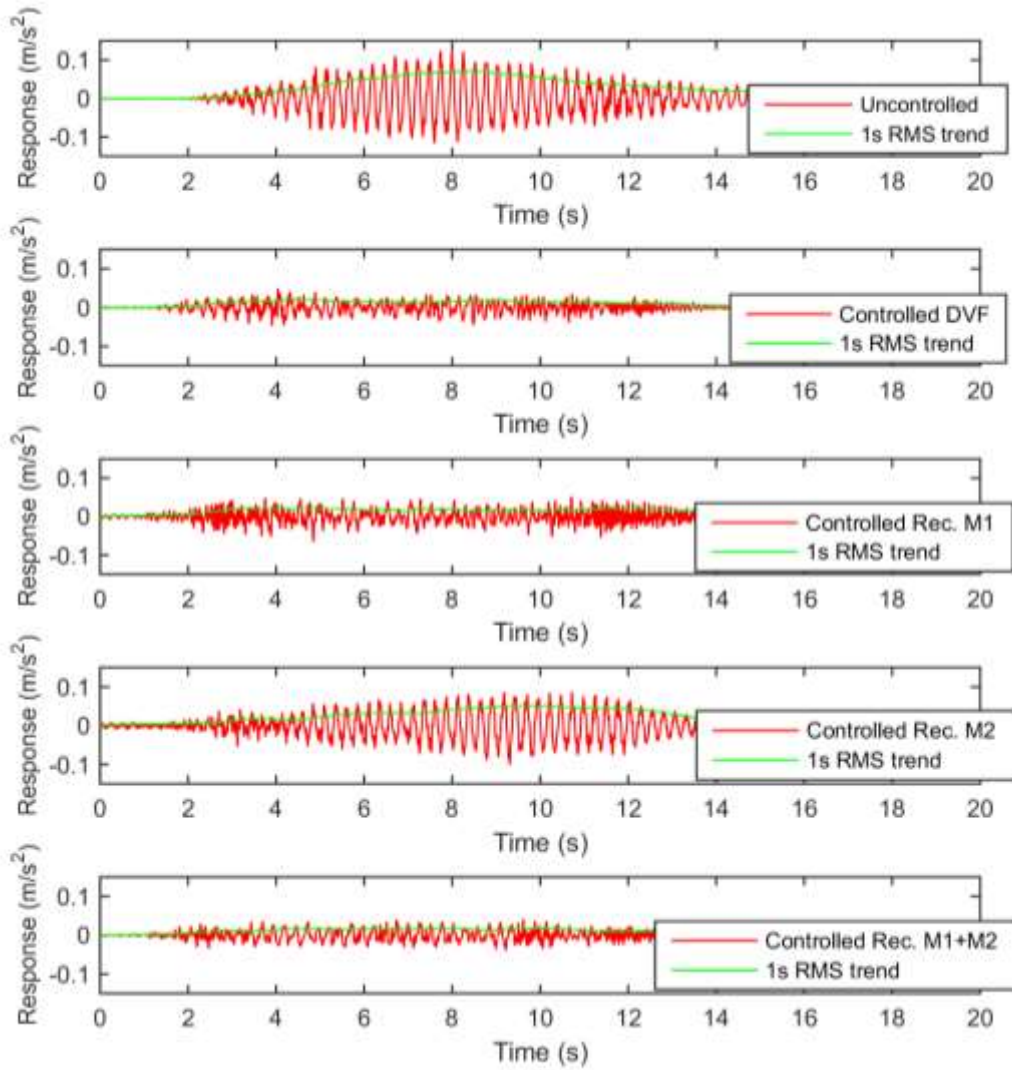
Figure 11 – Uncontrolled and controlled acceleration responses from experimental implementation for all responses at TP23

Table 5: Peaks of 1s running RMS acceleration responses for uncontrolled and controlled footbridge in experimental implementation

Mode	Acceleration responses at TP23 (m/s^2)	
		% reduction
Uncontrolled	0.0716	
DVF	0.0213	70.3
Receptance M1	0.0225	68.6
Receptance M2	0.0530	26.0
Receptance M1+M2	0.0181	74.6

The attenuations in target vibration modes of the structure observed from the FRF measurements range from 15-23 dB and are similar to those from the analytical predictions. Based on the results in Table 5, vibration mitigation performances between DVF and Receptance M1+M2 are quite comparable. Focusing control energy on the dominant mode of vibration of the footbridge prototype i.e. with receptance controller M1 still offers some desirable vibration mitigation performance for walking excitation tuned to excite resonance in this particular vibration mode. Poor performance is, however observed for Receptance controller M2 that focuses control energy on the

second vibration mode, which is understandable considering that the excitation is primarily at the frequency of the uncontrolled mode.

6 CONCLUSION

In this paper, the receptance based pole placement controller design approach has been investigated for designing appropriate velocity and acceleration feedback gains for vibration control of a footbridge prototype. This was designed in a SIMO controller configuration and the flexibility of realising additional control objectives beyond a purely DVF controller was seen. For example, the focus of control energy towards particular structural vibration modes. Comparative studies were carried out with a DVF controller in both numerical simulations and experimental implementations. There was good agreement between the analytical predictions and results from experimental implementations.

Further studies will develop multiple-input multiple-output controller configurations with the receptance based controller for control of pedestrian-induced vibration.

ACKNOWLEDGEMENT

REFERENCES

[1] Díaz, I. M., Pereira, E., Hudson, M. J. & Reynolds, P. Enhancing active vibration control of pedestrian structures using inertial actuators with local feedback control, *Engineering Structures*, 2012; **41**, 157–166.

[2] Hanagan, L. M., & Murray, T. M. Active Control Approach for Reducing Floor Vibrations, *Journal of Structural Engineering*, 1997; **123**(11), 1497–1505.

[3] Nyawako, D., Reynolds, P., & Hudson, M. J. Findings with AVC design for mitigation of human induced vibrations in office floors, *Conference Proceedings of the Society for Experimental Mechanics Series*, 2013; **39**(4), 37-44..

[4] Pereira, E., Díaz, I. M., Hudson, E. J., & Reynolds, P. Optimal control-based methodology for active vibration control of pedestrian structures, *Engineering Structures*, 2014; **80**, 153–162.

[5] Wonham, W.M. On pole assignment in multi-input controllable linear systems. *IEEE Transactions on Automatic Control*, 1967; **12***(6)*, 660–665.

[6] Davison, E.J. On pole assignment in linear systems with incomplete state feedback. *IEEE Transactions on Automatic Control*, 1970; **15**, 348–351.

[7] Ram, Y.K., & Mottershead, J.E. Receptance method in active vibration control, *AIAA Journal*, 2007; **45**(3), 562-567.

[8] Mottershead, J. E. Active vibration suppression by pole-zero placement using measured receptances, *Journal of Sound and Vibration*, 2008; **311**(3-5), 1391–1408.

[9] Ghandchi Tehrani, M., Elliott, R. N. R., & Mottershead, J. E. Partial pole placement in structures by the method of receptances: Theory and experiments, *Journal of Sound and Vibration*, 2010; **329**(24), 5017–5035.

[10] Tehrani, M. G., & Ouyang, H. Receptance-based partial pole assignment for asymmetric systems using state-feedback, *Shock and Vibration*, 2012, **19**, 1–8.

[11] British Standards Institution, BS6841: 1987 Measurement and evaluation of human exposure to whole-body mechanical vibration and repeated shock. *British Standard Guide*. Milton Keynes: British Standards Institution.

[12] ISO 2631-1-1997. Mechanical vibration and shock — Evaluation of human exposure to whole-body vibration - Part 1, General Requirements.